Many-Body Diagrammatic Expansion in a Kohn-Sham Basis: Implications for Time-Dependent Density Functional Theory of Excited States

I. V. Tokatly* and O. Pankratov

Lehrstuhl für Theoretische Festkörperphysik, Universität Erlangen-Nürnberg, Staudtstrasse 7/B2, 91054 Erlangen, Germany

(Received 17 August 2000)

We formulate diagrammatic rules for many-body perturbation theory which uses Kohn-Sham Green's functions as basic propagators. The diagram technique allows one to study the properties of the dynamic nonlocal exchange-correlation (xc) kernel f_{xc}. We show that the spatial nonlocality of f_{xc} is strongly frequency dependent. In particular, in extended systems the nonlocality range diverges at the excitation energies. This divergency is related to the discontinuity of the xc potential.

DOI: 10.1103/PhysRevLett.86.2078 PACS numbers: 71.10.–w, 31.15.Ew, 31.50.Df

Time-dependent density functional theory (TDDFT) [1] offers a possibility to extend a powerful density-functional formalism [2] to excited states of many-body systems [3–5]. A substantial improvement of excitation energies with respect to Kohn-Sham (KS) eigenvalues was obtained for atoms and molecules [3–6] using a variety of approximations for a dynamic exchange-correlation (xc) kernel $f_{\mathrm{xc}} = \delta v_{\mathrm{xc}}(\mathbf{r}, t)/\delta n(\mathbf{r}', t')$ (v_{xc} is an xc potential). However, in solids the wrong KS band gap remains unchanged regardless of the approximation used, albeit the dielectric function is on average improved [7].

This situation, as we show below, reflects an extremely nonlocal behavior (in $\mathbf{r}$ space) of $f_{\mathrm{xc}}(\mathbf{r}, \mathbf{r}')$ at excitation frequencies. The nonlocality range is as large as the system size and hence diverges in extended systems. None of the up-to-date approximations account for this behavior as they all employ the adiabatic (frequency-independent) xc kernels.

In this paper we develop a perturbative technique with KS Green's functions as the bare propagators. In essence, it is a diagrammatic expansion of the Sham-Schlüter equation [8], which maintains a correct electron density in every order of the perturbation theory. We find that at resonant frequencies the kernel f_{xc} is proportional to the discontinuity of v_{xc}. This explains the anomalous nonlocality of f_{xc}, since a constant shift of a potential due to an extra particle is felt by another particle anywhere in the system.

In the framework of TDDFT the excitation energies are commonly calculated [3,4,6] from the poles of the linear response function $\chi(\mathbf{r}, \mathbf{r}', \omega)$. The latter is related to the KS susceptibility $\chi_S(\mathbf{r}, \mathbf{r}', \omega)$ by

$$\chi(\omega) = \chi_S(\omega) + \chi_S(\omega)[V_C + f_{\mathrm{xc}}(\omega)]\chi(\omega), \quad (1)$$

where $V_C = e^2/|\mathbf{r} - \mathbf{r}'|$ is a Coulomb repulsion and the kernel f_{xc} enters as an additional dynamic interaction.

Alternatively, the poles of $\chi(\mathbf{r}, \mathbf{r}', \omega)$ can be found as the eigenvalues of a linearized equation for density matrix

$$[\omega - \hat{H}_S(\mathbf{r}_1) + \hat{H}_S(\mathbf{r}_2)]\delta\rho(\mathbf{r}_1, \mathbf{r}_2) - \rho_S(\mathbf{r}_1, \mathbf{r}_2)\int d\mathbf{r}[\tilde{V}_\omega(\mathbf{r}_1, \mathbf{r}) - \tilde{V}_\omega(\mathbf{r}, \mathbf{r}_2)]\delta\rho(\mathbf{r}, \mathbf{r}) = 0, \quad (2)$$

where $\tilde{V}_\omega = V_C + f_{\mathrm{xc}}(\omega)$, $\hat{H}_S(\mathbf{r})$ is the KS Hamiltonian, and $\rho_S(\mathbf{r}, \mathbf{r}') = \sum_j n_j \psi_j^*(\mathbf{r})\psi_j(\mathbf{r}')$ is the equilibrium KS density matrix with the KS orbitals $\psi_j^*(\mathbf{r})$. Equation (2) clearly shows that the correction to the KS excitation energies originates from the Hartree-type energy of the excitation-induced density fluctuation $\delta n(\mathbf{r}) = \delta\rho(\mathbf{r}, \mathbf{r})$. In the KS basis Eq. (2) takes the form

$$(\omega - \omega_{ij}^S)\delta\rho_{ij} - \gamma_{ij}\sum_{kl}\langle\Phi_{ij}|\tilde{V}_\omega|\Phi_{kl}\rangle\delta\rho_{kl} = 0, \quad (3)$$

where $\omega_{ij}^S = E_i^S - E_j^S$ is a KS excitation energy, $\gamma_{ij} = n_i - n_j$ is the difference of the occupation numbers, and $\Phi_{ij}(\mathbf{r}) = \psi_i^*(\mathbf{r})\psi_j(\mathbf{r})$. For electron-hole ($e$-$h$) excitations the ordinary perturbation theory gives the energy shift $\Delta\omega_{ij} = \omega_{ij} - \omega_{ij}^S$ in the first order as

$$\Delta\omega_{ij}^{(1)} = \langle\Phi_{ij}(\mathbf{r})|V_C(\mathbf{r}, \mathbf{r}') + f_{\mathrm{xc}}(\mathbf{r}, \mathbf{r}', \omega_{ij}^S)|\Phi_{ij}(\mathbf{r}')\rangle, \quad (4)$$

which is identical to the result of the first-order Laurent expansion of $\chi(\mathbf{r}, \mathbf{r}', \omega)$ [3]. Equations (2) and (3) are equally valid for finite and for extended systems, whereas the perturbative result (4) requires that states i and j are nondegenerate (see below). In particular, Eq. (4) gives a shift of the energy gap in a bulk semiconductor with nondegenerate band edges.

Let us consider dependence of the first-order correction (4) on the size of a system $L \sim V^{1/3}$ at fixed average density N/V. As $\Phi_{ij}(\mathbf{r})$ contains a normalization factor $1/V$, the first term in Eq. (4) is proportional to e^2/L. This is the Coulomb energy of the density variation due to an e-h excitation, which is infinitesimally small in extended systems. The second term crucially depends on the nonlocality of f_{xc}, i.e., on the extension of an xc hole. At $\omega = 0$ the nonlocality range is about the interparticle distance $l \sim (V/N)^{1/3}$. This feature is reproduced by the popular optimized effective potential (OEP) approximation [3],

 0031-9007/01/86(10)/2078(4)$15.00

whereas in adiabatic local density approximation (LDA) [9] $f_{\rm xc}$ is a point interaction. Assuming that at resonance frequency $f_{\rm xc}(\omega_{ij})$ has a similar nonlocality we find that the second term in Eq. (4) is proportional to $1/N$ and vanishes as L^{-3} (see, however, [10]). Thus *any* xc kernel which is finite and decays at infinity does not contribute to ω_{ij} in extended systems. Using the many-body perturbative approach formulated below, we show that a nonvanishing xc correction arises due to the divergency of the nonlocality scale of $f_{\rm xc}(\omega_{ij})$. We employ the Matsubara formalism at nonzero temperature T which enables us to obtain any physical retarded function through analytic continuation [11]. Assuming that the xc potential $v_{\rm xc}(\mathbf{r})$ and the ground state density are known, we represent the Hamiltonian of a system as a sum of the KS Hamiltonian $\hat{H}_S$ and the perturbation $\hat{V}$, where

$$\hat{V} = \hat{W}' - \sum_{k=1}^{\infty} \int d\mathbf{r}\, v_{\rm xc}^{(k)}(\mathbf{r})\hat{n}(\mathbf{r})\,. \qquad (5)$$

In Eq. (5) $\hat{W}'$ is a two-particle interaction with the Hartree part being subtracted, $\hat{n}(\mathbf{r})$ is a density operator, and we assume that the xc potential $v_{\rm xc}$ can be expanded in a power series $v_{\rm xc} = \sum_{k=1}^{\infty} v_{\rm xc}^{(k)}$, where $v_{\rm xc}^{(k)} \sim e^{2k}$.

Following the standard procedure [11] we define the Green's function

$$G(X, X') = -\langle T_\tau \Psi_S(X)\Psi_S^+(X')\hat{\sigma}\rangle / \langle\hat{\sigma}\rangle\,, \qquad (6)$$

where $X = (\mathbf{r}, \tau)$ (τ is an imaginary time), $\Psi_S(X)$ is a field operator in a KS interaction representation, and $\hat{\sigma}$ is a Matsubara S-matrix [11] which corresponds to the perturbation $\hat{V}$ of Eq. (5). The angular brackets in Eq. (6) denote averaging over the KS equilibrium state.

A perturbative expansion of $G(X, X')$ contains along with the pair interaction graphs the diagrams related to the scattering by "external" potentials $v_{\rm xc}^{(k)}$. To achieve a closed scheme one needs a complementary graphical representation of $v_{\rm xc}(\mathbf{r})$, which can be obtained from the condition of the density conservation. The Green's function (6) can be written in the form $G = G_S + \sum_{k=1}^{\infty} G^{(k)}$, where G_S is a KS Green's function and $G^{(k)}$ is a kth order correction. As the KS system possesses an exact density, the variation of the density due to interaction (5) must vanish. Applying this requirement in every order we obtain

$$\delta n^{(k)}(\mathbf{r}) = T \sum_{n=-\infty}^{\infty} G^{(k)}(\mathbf{r}, \mathbf{r}, \omega_n) = 0\,, \qquad (7)$$

where $\omega_n = \pi T(2n + 1)$. Equation (7) is equivalent to the well-known Sham-Schlüter equation [8,12]. A successive solution of Eq. (7) allows one to construct $v_{\rm xc}^{(k)}$ for every k. For example, the first-order correction $G^{(1)}$ is presented in Fig. 1a, where the solid line is the KS Green's function and the dashed line is the Coulomb interaction. Substituting $G^{(1)}$ into Eq. (7) we get $v_{\rm xc}^{(1)}$ as shown in Fig. 2a, where the wiggled line stands for the inverse KS response function $\chi_S^{-1}(\mathbf{r}, \mathbf{r}')$. The final first-order correction to the Green's function is shown in Fig. 1b. Note

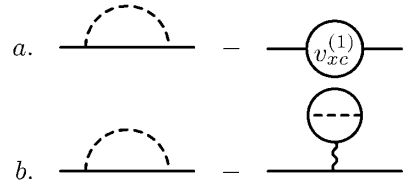

FIG. 1. First-order corrections to the Green's function.

that $v_{\rm xc}^{(1)}$ (Fig. 2a) exactly corresponds to the x-only OEP v_x. Given $v_{\rm xc}^{(1)}$ we solve Eq. (7) for $k = 2$ and obtain eight graphs for $v_{\rm xc}^{(2)}$ (Figs. 2b–2i). From the further iterations we deduce the following diagrammatic rules for $v_{\rm xc}$ in arbitrary order: (i) Draw all graphs for density according to the usual rules [11] and attach wiggled lines to the external point of each graph. (ii) Whenever it is possible separate the graphs into two parts by cutting two fermionic lines. Join the external fermionic lines of these parts and connect them by the wiggled line. Do not cut lines attached to the external wiggled line. (iii) If a new graph is separable, repeat (ii). (iv) If several cross sections are possible, repeat (ii) and (iii) for all of them. (v) Leave only nonequivalent graphs. For example, graphs (a)–(e) in Fig. 2 appear according to (i). Graph (f) is obtained from (d) applying (ii). Graphs (g)–(i) originate from (e) by the successive application of (ii)–(v).

Given a diagrammatic representation for $v_{\rm xc}$ we can easily construct a graphical expansion for any quantity, e.g., for one particle Green's function, a response function, or an energy. We find that the series for the energy coincides with the expansion obtained in a different context in Ref. [13]. As the diagrammatic expansion is derived maintaining the exact density in every order, the series for $v_{\rm xc}$ is in fact a graphical representation of the Görling-Levy perturbation theory (GLPT) [14]. An obvious advantage of the graphical method is a possibility to construct $v_{\rm xc}^{(k)}$ for every k in a transparent form.

An important feature of the KS-based diagram technique is that every irreducible self-energy insertion $\Sigma(\mathbf{r}, \mathbf{r}')$ is accompanied by the *local* counterterm which has the structure of the average of Σ: $(G_S\Sigma G_S)(G_S G_S)^{-1}$. This term guarantees the density conservation and *locally* reduces the effective field Σ. The first-order correction (Fig. 1b) gives an example of this compensation. It is interesting to note

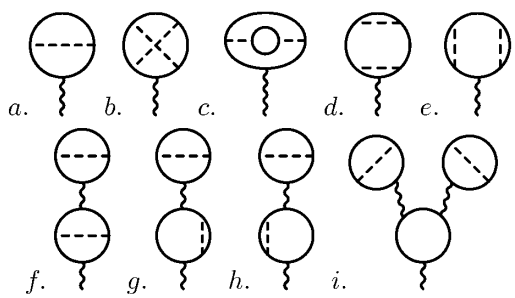

FIG. 2. First- (a) and second-order (b)–(i) diagrams for xc potential.

that the standard diagram technique can be reformulated in a similar fashion. One has to explicitly introduce a correction to the chemical potential to compensate the change of the total number of particles (averaged density) in every order of the perturbation theory. This leads to similar, but spatially averaged, counterterms. Apparently the local compensation in the KS-based technique is more efficient. This means that KS particles are much closer to the true quasiparticles than bare electrons.

Our graphical method has an obvious connection to the GW approximation [15]. Let us collect in every order of the perturbation theory only the bubble diagrams (e.g., the graph in Fig. 2c) and sum them up. The corresponding correction to the Green's function is still given by Fig. 1b, but with the RPA-screened interaction. While the first graph in Fig. 1b is exactly the GW self-energy, the second one deviates from the common GW prescription. Instead of subtraction of the whole $v_{\rm xc}$, one has to use an *approximate* $v_{\rm xc}$ (even if the exact $v_{\rm xc}$ is known). This is a requirement of internal consistency and facilitates the density conservation. From this point of view it is clear that the KS eigenvalues describe well quasiparticles in metals (e.g., the shape of the Fermi surface), but not in semiconductors. Indeed, for a short-ranged screened interaction in metals the first (nonlocal) and the second (local) term in Fig. 1b almost cancel (they would cancel exactly for a point interaction). Conversely, in insulators there is no pronounced cancellation since the interaction is long ranged. As a result, the correction to the KS energies gets larger the larger the gap is.

To study the e-h excitations one has to consider the linear response function $\chi(\mathbf{r}, \mathbf{r}', \omega_n)$. An integral equation for this function,

$$\chi(\omega_n) = \tilde{\chi}(\omega_n) + \tilde{\chi}(\omega_n) V_C \chi(\omega_n), \tag{8}$$

contains irreducible polarization operator $\tilde{\chi}(\omega_n)$. We split $\tilde{\chi}(\omega_n)$ into two parts: $\tilde{\chi}(\omega_n) = \chi_S(\omega_n) + \Pi(\omega_n)$, where $\Pi(\omega_n)$ includes all (self-energy and vertex) corrections to the irreducible susceptibility $\tilde{\chi}(\omega_n)$. The first-order corrections to $\chi(\omega_n)$ are shown in Fig. 3, where the first four terms correspond to the first-order correction $\Pi^{(1)}(\omega_n)$. Thus the total response function in the first order is

$$\chi(\omega_n) \approx \chi_S(\omega_n) + \Pi^{(1)}(\omega_n) + \chi_S(\omega_n) V_C \chi_S(\omega_n). \tag{9}$$

The graphs in Fig. 3 display the physical meaning of all corrections to the e-h excitation energy. The first two diagrams as well as the third and the fourth graphs are the self-

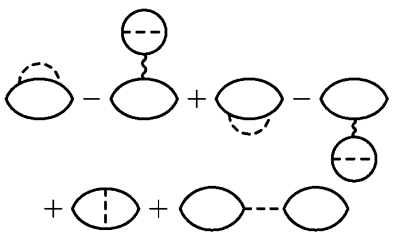

FIG. 3. First-order corrections to the response function.

energy corrections for an electron and a hole, respectively. The last term is the Coulomb energy of the excitation-induced charge density, while the fifth graph is the e-h interaction. Summation of the ladder diagrams in the e-h loop would allow one to include excitonic effects, which we do not consider here.

Performing summation over frequencies with subsequent analytic continuation in the first five diagrams in Fig. 3 we obtain $\Pi^{(1)}(\omega)$ close to the excitation frequency ω_{ij}^S:

$$\Pi^{(1)}(\omega) = \Phi_{ij}(\mathbf{r}) \Phi_{ij}^*(\mathbf{r}') \frac{\gamma_{ij} \Delta_{ij}}{(\omega - \omega_{ij}^S)^2}, \tag{10}$$

$$\begin{aligned} \Delta_{ij} = {} & \langle \psi_i(\mathbf{r}) | v_F(\mathbf{r}, \mathbf{r}') - v_x(\mathbf{r}) \delta(\mathbf{r} - \mathbf{r}') | \psi_i(\mathbf{r}') \rangle \\ & - \langle \psi_j(\mathbf{r}) | v_F(\mathbf{r}, \mathbf{r}') - v_x(\mathbf{r}) \delta(\mathbf{r} - \mathbf{r}') | \psi_j(\mathbf{r}') \rangle \\ & - \langle \Phi_{ii}(\mathbf{r}) | V_C(\mathbf{r}, \mathbf{r}') | \Phi_{jj}(\mathbf{r}') \rangle. \end{aligned} \tag{11}$$

In Eq. (11) $v_F(\mathbf{r}, \mathbf{r}')$ is the Fock nonlocal potential and $v_x(\mathbf{r})$ is the local exchange potential or OEP. Apparently $\gamma_{ij}\Delta_{ij}$ is a shift of the excitation energy due to the first five graphs in Fig. 3. The last graph gives a correction which is the first term in Eq. (4). The total correction $\Delta\omega_{ij}^{(1)} = \gamma_{ij}(\Delta_{ij} + \langle \Phi_{ij} | V_C | \Phi_{ij} \rangle)$ coincides with the first-order GLPT [16,17]. With the increase of a system volume the last term in Eq. (11) (the energy of the e-h interaction) vanishes as e^2/L. Conversely, the first two terms remain finite (of the order of e^2/l) and describe, e.g., an exchange shift of the band gap of a semiconductor.

The above results can be restated in terms of TDDFT. In the linear approximation, i.e., after the first iteration, Eq. (1) yields

$$\chi(\omega_n) \approx \chi_S(\omega_n) + \chi_S(\omega_n) [V_C + f_{\rm xc}(\omega_n)] \chi_S(\omega_n). \tag{12}$$

A comparison to Eq. (9) leads to the following relation:

$$f_{\rm xc}(\omega) = \chi_S(\omega)^{-1} \Pi^{(1)}(\omega) \chi_S(\omega)^{-1}. \tag{13}$$

As the linear $v_{\rm xc}^{(1)}$ is simply the x-only OEP (Fig. 2a), Eq. (13) should provide a dynamical OEP kernel $f_x^{\rm OEP}(\omega)$. Indeed, a functional differentiation of the graph Fig. 2a versus density yields Eq. (13). A similar expression for $f_x^{\rm OEP}(\omega)$ was derived in [18] by solving the dynamic OEP equations. Our approach gives a graphical interpretation of this result.

At any nonresonant frequency, e.g., in statics $\omega = 0$, the nonlocality range of $f_{\rm xc}$ Eq. (13) is about an interparticle distance l. The correction to the excitation energies Eq. (4) depends, however, on the kernel at resonance $f_{\rm xc}(\omega_{ij}^S)$. Let us consider a spatial extension of this kernel using Eq. (13). To calculate $\chi_S^{-1}(\omega)$ at resonance we write $\chi_S = \gamma_{ij}\Phi_{ij}(\mathbf{r})\Phi_{ij}(\mathbf{r}')/(\omega - \omega_{ij}^S) + \chi_r(\mathbf{r}, \mathbf{r}')$, where χ_r is a regular part. Substituting $\Pi^{(1)}(\omega)$ (10) to Eq. (13) and performing calculations we arrive at the following result:

$$f_{\mathrm{xc}}(\mathbf{r},\mathbf{r}',\omega_{ij}) = \Delta_{ij}\,\frac{\int d\mathbf{r}_1\, d\mathbf{r}_2\, \chi_r^{-1}(\mathbf{r},\mathbf{r}_1)\Phi_{ij}(\mathbf{r}_1)\Phi_{ij}^{*}(\mathbf{r}_2)\chi_r^{-1}(\mathbf{r}_2,\mathbf{r}')}{\langle\Phi_{ij}^{*}(\mathbf{r}_2)|\chi_r^{-1}(\mathbf{r}_2,\mathbf{r}_1)|\Phi_{ij}(\mathbf{r}_1)\rangle^2}\,. \tag{14}$$

The spatial scale of $f_{\mathrm{xc}}(\mathbf{r},\mathbf{r}',\omega_{ij})$ is governed by functions $\Phi_{ij}(\mathbf{r})$ which extend over the volume. Hence the nonlocality range of the resonant f_{xc} is simply a system size, which facilitates a finite xc contribution $\langle\Phi_{ij}|f_{\mathrm{xc}}(\omega_{ij})|\Phi_{ij}\rangle = \Delta_{ij}$ in Eq. (4). This result was considered in Ref. [17] as an evidence of equivalence of GLPT and TDDFT. We emphasize that this equivalence holds only for a dynamic xc kernel at resonant frequency and is not fulfilled by any static approximation.

For simplicity we assumed that the transition at ω_{ij} connects nondegenerate states. In a degenerate case the result is analogous to Eq. (14) but contains a sum over all e-h states with the same ω_{ij} [19]. For a finite degeneracy (e.g., a semiconductor with degenerate band edges) the reasoning of (14) regarding a nonlocality of f_{xc} remains unaltered. A continuous degeneracy (as for states above the band edges) requires a special consideration which will be published elsewhere. The inherent long rangedness of $f_{\mathrm{xc}}(\omega)$ at frequencies above the e-h continuum has been pointed out in [20]. The nonlocality of (14) is, however, of a different nature. It occurs exactly at resonance frequencies and consequently affects the e-h excitation energies.

It is straightforward to construct a kernel $f_{\mathrm{xc}}^{\mathrm{GW}}(\omega)$ which reproduces the first-order GW result. One has to replace $\Pi^{(1)}(\omega)$ in Eq. (13) by $\Pi^{(1)}_{\mathrm{scr}}(\omega)$ which is defined by the first four graphs in Fig. 3, but with the RPA-screened interaction. TDDFT formalism with this $f_{\mathrm{xc}}^{\mathrm{GW}}(\omega)$ exactly reproduces the GW approach. For a semiconductor with the band gap E_g, the xc kernel at $\omega = E_g$, which is responsible for the band gap correction, is given by Eq. (14) with $\Delta_{ij} = \Delta_{N+1} - \Delta_{N-1}$. Here Δ_{N+1} (Δ_{N-1}) are the discontinuities of the xc potential upon addition (removal) of a particle. The fundamental relation of f_{xc} at resonant frequency to the discontinuity of v_{xc} has a simple physical interpretation. The jump of v_{xc} signifies a constant shift of a potential throughout the system due to addition of one particle. It means that another probe particle interacts with the first one anywhere in a system. This should be interpreted as an xc interaction with a length scale of the size of a system and with an amplitude equal to the discontinuity of v_{xc}. Importantly, this result holds only at resonant frequency where a real creation of the e-h pair takes place. The arguments above show that not only any static approximation but also any LDA-based dynamic approximation (including any gradient corrections) for f_{xc} cannot provide consistent results for excitation energies and a construction of explicit orbital- and frequency-dependent functionals similar to Eq. (13) is required. An alternative is a direct calculation of the irreducible polarization operator using the diagram method outlined above. This formally allows us to express excitation energies as functionals of the KS orbitals and consequently of the ground state density.

The work of I. T. was supported by the Alexander von Humboldt Foundation and partly by the Russian Federal Program "Integration."

*On leave from Moscow Institute of Electronic Technology, Zelenograd, 103498 Russia.
Email address: ilya.tokatly@physik.uni-erlangen.de

[1] E. Runge and E. K. U. Gross, Phys. Rev. Lett. **52**, 997 (1984).
[2] R. M. Dreizler and E. K. U. Gross, *Density-Functional Theory* (Springer-Verlag, Berlin, 1990), and references therein.
[3] M. Petersilka, U. J. Gossmann, and E. K. U. Gross, Phys. Rev. Lett. **76**, 1212 (1996).
[4] K. Burke and E. K. U. Gross, in *Density Functionals: Theory and Applications,* edited by D. Joubert (Springer, Berlin, 1998).
[5] R. Singh and B. M. Deb, Phys. Rep. **311**, 47 (1999).
[6] M. Petersilka, E. K. U. Gross, and K. Burke, cond-mat/0001154.
[7] F. Kootstra, P. L. de Boeij, and J. G. Snijders, J. Phys. Chem. **112**, 6517 (2000).
[8] L. J. Sham and M. Schlüter, Phys. Rev. Lett. **51**, 1888 (1983).
[9] A. Zangwill and P. Soven, Phys. Rev. Lett. **45**, 204 (1980).
[10] In addition to the short-ranged part, the static f_{xc} in extended systems with a gap has a tail $\sim 1/|\mathbf{r} - \mathbf{r}'|$ [Ph. Ghosez, X. Gonze, and R. W. Godby, Phys. Rev. B **56**, 12 811 (1997)]. This gives an additional contribution $\sim 1/L$ to Eq. (4).
[11] E. M. Lifshitz and L. P. Pitaevskii, *Statistical Physics, Part 2: Theory of the Condensed State,* Course of Theoretical Physics Vol. 9 (Pergamon, New York, 1980).
[12] The diagrammatic interpretation of the Sham-Schlüter equation and the first-order solution (equivalent to the graph Fig. 1a) was given in L. J. Sham, Phys. Rev. B **32**, 3876 (1985); see also B. Farid, Philos. Mag. B **76**, 145 (1997); Solid State. Commun. **104**, 227 (1997).
[13] R. Fukuda *et al.,* Prog. Theor. Phys. Suppl. **121**, 1 (1995); M. Valiev and G. W. Fernando, cond-mat/9702247.
[14] A. Görling and M. Levy, Phys. Rev. A **50**, 196 (1994).
[15] L. Hedin, Phys. Rev. **139**, A796 (1965).
[16] A. Görling, Phys. Rev. A **54**, 3912 (1996).
[17] X. Gonze and M. Scheffler, Phys. Rev. Lett. **82**, 4416 (1999).
[18] A. Görling, Int. J. Quantum Chem. **69**, 265 (1998).
[19] The derivation of $f_{\mathrm{xc}}(\omega_{ij})$ in a degenerate case requires an invertibility of the matrix $M_{\mu\nu} = \langle\Phi_\mu|\chi_r^{-1}|\Phi_\nu\rangle$, where μ, ν label the degenerate states. In spatially homogeneous systems determinant of this matrix vanishes. This means that a singular nonlocality of $f_{\mathrm{xc}}(\omega_{ij})$ occurs only in inhomogeneous systems.
[20] G. Vignale and W. Kohn, Phys. Rev. Lett. **77**, 2037 (1996).